JOURNAL OF AIRCRAFT
Vol. 37, No. 5, September–October 2000

Prediction Measurement of a Low-Frequency Harmonic Noise of Hovering Model Helicopter Rotor

F. H. Schmitz*
University of Maryland, College Park, Maryland 20742
H. R. Aggarwal†
Helicopter Aerodynamics and Noise, Mountain View, California 94040
and
D. A. Boxwell‡
NASA Ames Research Center, Moffett Field, California 94035

Far-field acoustic data for a model helicopter rotor have been gathered in a large, open-jet, acoustically treated wind tunnel with the rotor operating in hover and out of ground effect. The four-bladed Boeing 360 model rotor with advanced airfoils, planform, and tip shape was tested over a range of conditions typical of today's modern helicopter main rotor. Near in-plane acoustic measurements were compared with two independent implementations of classical linear acoustic theory. Measured steady thrust and torque were used together with a free-wake analysis (to predict the thrust and drag distributions along the rotor radius) as input to this first-principles theoretical approach. Good agreement between theory and experiment was shown at low frequencies (for both amplitude and phase) at those measurement locations where low-frequency facility distortions were minimal.

Nomenclature

a_0	=	speed of sound
C_Q	=	rotor torque coefficient
C_T	=	rotor thrust coefficient
D	=	rotor diameter
$\mathrm{d}S$	=	elemental surface area of the rotating blade
$\mathrm{d}V$	=	elemental fluid volume
M_H	=	rotor hover tip Mach number
M_r	=	component of the Mach number of the moving source in the direction of the observer
n	=	unit normal to the rotor blade surface
P	=	fluid pressure
P_0	=	undisturbed fluid pressure
p'	=	acoustic pressure $(P - P_0)$
R	=	rotor radius
R_0	=	distance from the rotor hub to the observer
r	=	distance from the moving source to the fixed observer
T_{ij}	=	Lighthill stress tensor
u_{ij}	=	fluid velocity perturbation stress tensor
u_n	=	perturbation velocity normal to the surface of the blade
V	=	forward velocity of the helicopter
V'	=	total velocity at the rotor blade, $\{(\Omega r)^2 + V^2\}^{1/2}$
v	=	rotor induced velocity
X, Y, Z	=	Duits Nederlandse Wind Tunnel acoustic measurement coordinate system
$\boldsymbol{x}$	=	spatial position of the observer
$\boldsymbol{y}$	=	spatial position of a moving source
α	=	angle between the rotor tip-path-plane and a line drawn from the hub to the observer
θ	=	rotor blade pitch angle
μ	=	rotor advance ratio, $(V/\Omega R)$
ρ	=	density of the fluid
ρ_0	=	undisturbed reference density of the fluid
ρ'	=	perturbation density of the fluid, $(\rho - \rho_0)$
σ	=	rotor solidity
Ω	=	rotor rotational rate

Introduction

DESIGNING rotorcraft for low noise levels from a first-principles approach requires accurate theoretical methods that faithfully duplicate the physical sources of noise and their radiated levels. This implies that the theoretical acoustic modeling must be quantitatively accurate to a sufficient level of detail so that the effects of specific rotor design changes are reflected in the radiated noise levels. Some success has been achieved in predicting large overall noise level changes resulting from gross design parameter changes such as rotor-tip Mach number, integrated thrust of the rotor, and rotor blade thickness. However, many detailed rotor design changes, such as tip shape effects, rotor twist distributions, and rotor airfoil design, that have been based on theory have not been entirely successful, partly because the basic theoretical methods have not been validated over the conditions under which they have been applied.

The most straightforward experiment to validate acoustic theory for rotorcraft also appears to be the simplest to undertake, that of a hovering rotor or propeller. In 1952, Hubbard and Lassiter measured the far-field noise of a propeller that was mounted on a static thrust stand with its thrust axis horizontal.[1] Measured time histories of the noise both in and out of the plane of rotation were reported. Linear theory was used to predict the harmonic noise levels. (The blade forces were modeled by acoustic dipoles, and blade-thickness effects were neglected.) Agreement within 6 dB for the first 12 harmonics was reported for a tip Mach number of 0.75. In general, theory underpredicted the measured harmonic noise levels. Unfortunately, no quantitative time history comparison between theory and experiment was attempted, and so the relative importance of blade thickness effects could not be ascertained. In addition, the nearby ground plane was not acoustically treated; as a result ground reflections tended to distort the measured time histories. Despite these limitations, this pioneering set of noise measurements did validate the Gutin theory[2] to within 6 dB (factor of two) for steady hovering harmonic noise.

Received 11 December 1998; revision received 16 February 2000; accepted for publication 17 February 2000.

*Martin Professor of Rotorcraft Acoustics, Department of Aerospace Engineering. Associate Fellow AIAA.
†President, 3374 Tryna Drive; currently retired.
‡Research Scientist, U.S. Army Aeroflightdynamics Directorate, U.S. Army Aviation and Missile Command.

Finding high-quality acoustic data for hovering helicopter rotors is also quite difficult. There are many sources of noise on a conventional helicopter other than the main and tail rotors that contribute to the measured time histories. In addition, aerodynamic unsteadiness (which itself can introduce additional noise sources), atmospheric effects, and ground reflection problems complicate the measurement problem. These undefined variables tend to reduce the correlation between theory and measurement. In an effort to control the unsteadiness of the hovering rotor and place the rotor itself effectively out of ground effect, Leverton measured the noise of an inverted full-scale helicopter main rotor (thrust vector pointing down).[3] Far-field noise measurements were made by using tethered balloons to hold the microphones in position on an arc over the top of the rotor. The resulting data were quite steady and were at first thought to be representative of a large, clean rotor. However, turbulence near the ground was ingested into the inverted rotor creating additional noise sources, which tended to reduce the usefulness of the data. Many other full-scale experiments have been run on isolated main rotors in efforts to validate theory,[4–9] but ground reflections, atmospheric effects, and the operation of the rotors in aerodynamic ground effect have introduced experimental uncertainties in the data that have made quantitative validation of theory quite difficult.

High-quality steady hovering acoustic data were gathered at model scale by Boxwell et al.[10] An untwisted one-seventh-scale UH-1H helicopter two-bladed rotor was operated at Mach numbers from 0.8 to 1.0 out of ground effect in a specially designed anechoic hover chamber. To keep recirculation effects to a minimum, thrust levels near zero were maintained throughout the Mach number range. The testing chamber was designed to be anechoic down to 110 Hz, thus minimizing acoustic reflections from low-frequency rotor harmonic noise while effectively eliminating reflections from higher frequency rotor noise. Because high-frequency impulsive noise was the dominant noise source at these high effective tip Mach numbers, the measuring chamber was effectively anechoic; that is, measurements were not distorted by reflection from nearby surfaces. The results of comparing these high-quality data to a first-principle acoustic analysis revealed the limitations of linear theory. At hovering tip Mach numbers of 0.8–0.88 for the UH-1H rotor, linear theory predicted the correct waveform of the time history but underpredicted the peak amplitude by a factor of two. It was also shown that the in-plane noise levels were dominated by rotor-thickness effects and only slightly affected by the thrust and torque of the rotor. At tip Mach numbers exceeding 0.88, the noise radiation became dominated by nonlinear acoustic effects that could not be described by simple linear acoustic theories.

In the last decade and since the completion of this experiment, there have been several acoustic wind-tunnel programs that have concentrated on qualitatively measuring helicopter noise. These programs have focused on the most offensive sources of rotorcraft noise/annoyance, which are dominated by high-speed impulsive noise (which occurs at high forward speeds) and blade–vortex interaction noise (which normally occurs during descending flight).[11–13] Although not usually highlighted, lower-frequency harmonic noise of hovering rotorcraft can also be important for some military operations where acoustic detection is to be achieved or avoided. Because of potential military uses, publication of acoustic data on existing or future planned military rotor systems has not been encouraged, thus limiting the available data sets that can be used for theory/code validation. However, because no military production of the Boeing 360 model-rotor system is foreseen, publication of acoustic data in simulated hovering conditions for this rotor has been permitted. This military sensitivity also explains why there have been no low-frequency hovering acoustic data reported in the literature in the last decade.

In this paper, noise measurements made during hover are compared with linear theory results over the Mach number range typical of a modern four-bladed helicopter rotor. The known problems of aerodynamic recirculation, acoustic reflections from nearby surfaces, and the proximity of the ground to the rotor were minimized by careful test design. The model rotor was mounted in a large acoustically treated room [the Duits Nederlandse Wind Tunnel (DNW) open-jet wind tunnel] out of ground-acoustic theory validation of a hovering helicopter rotor and is compared with linear theory at several elevation angles and distances for several thrusts and Mach numbers typical of a modern hovering helicopter.

Theoretical Modeling

The noise that is radiated by a body in arbitrary motion is mathematically represented by the well-known integral equation

$$4\pi a_0^2\rho'(\boldsymbol{x},t) = \frac{\partial}{\partial t}\int\underbrace{\left[\frac{\rho_0 u_n}{r|1-M_r|}\right]_{\mathrm{ret}}}_{\text{monopole}}\mathrm{d}S(\boldsymbol{y}) - \frac{\partial}{\partial x_i}\int\underbrace{\left[\frac{P_{ij}n_j}{r|1-M_r|}\right]_{\mathrm{ret}}}_{\text{dipole}}\mathrm{d}S(\boldsymbol{y}) + \frac{\partial^2}{\partial x_i\partial x_j}\int\underbrace{\left[\frac{T_{ij}}{r|1-M_r|}\right]_{\mathrm{ret}}}_{\text{quadrupole}}\mathrm{d}V(\boldsymbol{y}) \qquad (1)$$

where $T_{ij} = \rho u_i u_j + P_{ij} - a_0^2\rho'\delta_{ij}$. This equation was derived from first principles in Ref. 14 and has been expanded by many researchers. Acoustic density is explicitly expressed in terms of integrals over the body surface and the surrounding volume in a reference frame moving with the body surface. Note that Eq. (1) is in the strictest sense a nonlinear integral equation over all space. Often, the right-hand side integrals are assumed to be bounded and finite and basically independent of the left-hand side. Under these conditions, all three terms in Eq. (1) can be interpreted as sources of rotorcraft noise. This first term represents the noise that is caused by the body displacing fluid as it traverses its arbitrary path; the second term represents the noise due to body surface pressures pushing on the fluid; and the third term describes the noise that is due to fluid stress, which becomes important at transonic Mach numbers. For acoustics, $p' = a_0^2\rho'$ so that the left-hand side of Eq. (1) can be interpreted as acoustic pressure p'.

Only the far-field noise that is generated by thickness effects and by the steady forces of a hovering rotor turning at low rotational Mach numbers are considered in this paper. It is also assumed that the blade surface pressure is known so that the far-field acoustic pressure can be obtained explicitly by simply evaluating Eq. (1) with known values of the blade-thickness distribution and surface pressure. Of course, all sources must be tracked in the circular path of the hovering rotor, with particular attention given to source emission and receiver times, respectively. A sketch of the geometry of a simple hovering rotor is shown in Fig. 1. Depicted are thickness (monopole) and pressure (dipole) sources on a single rotating blade. These thickness and pressure effects can be thought of as distributions of rotating monopoles and steady dipoles, respectively, and are described mathematically by the first and second terms of Eq. (1). According to Eq. (1), the radiated noise due to thickness and steady loading is simply a time and spatial derivative, respectively, of the summation of the thickness and pressure source terms taken at the correct retarded time. In essence, a simple, linear, three-dimensional

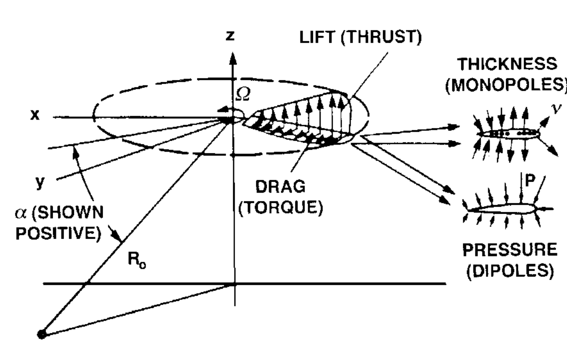

Fig. 1 Geometry of hovering rotor with steady thickness and loading distributions.

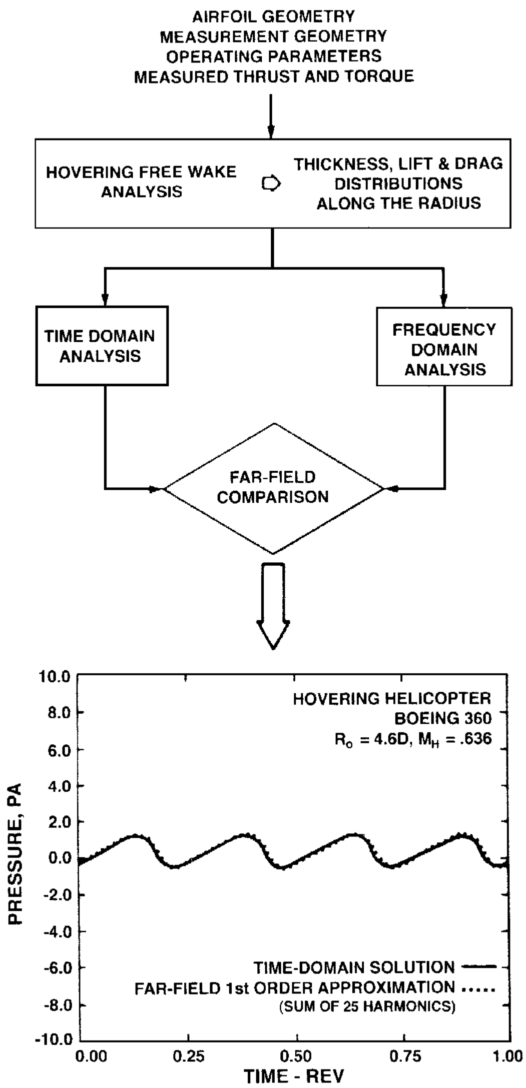

Fig. 2 Comparison of far-field noise predicted by independent time and frequency-domain computational methods.

wave equation is being solved. The retarded-time operator keeps track of source emission and receiver times.

At low rotational Mach numbers, it is often assumed that the pressures can be integrated chordwise and represented by a spanwise line of rotating point forces. This compact acoustic source approximation has been used extensively by early propeller-noise researchers and is valid when the wavelength of the radiated sound of interest is much larger than the characteristic dimension of the source (blade chord). Because we are only interested in long-wavelength, low-frequency sound, this is a valid approximation for the sound radiated by a hovering rotor with a low tip Mach number. These integrated forces (lift and drag) distributed along the radius of the blade at the one-quarter-chord line are also illustrated in Fig. 1.

Despite these simplifications, the rotating geometry of the hovering rotor still makes the computation of the noise a nontrivial numerical evaluation that is subject to all of the normal errors of programming. To establish the accuracy of the computations, two separate evaluations of Eq. (1) were performed, and the results cross-checked before a comparison with experiment was attempted. The numerical evaluation began with the specification of airfoil geometry, the measurement geometry, and the rotor operating parameters of the Boeing 360 model-rotor. These were then used to run a hovering free-wake analysis to obtain the lift and drag distributions along the radius of the hovering rotor for each condition. This process is shown in Fig. 2. The measured values of thrust and torque were then used to scale the thrust and drag distribution levels as a function of radius for each test condition. These data, along with the known thickness distributions along the radius, were used as input to two separate acoustic codes to predict the radiated noise independently.

The aerodynamic loading distributions of this hovering rotor is shown in Fig. 3. The lift and drag distributions along the radius leave a very complicated wake system that has a large influence on those very distributions. The free-wake system of Ref. 15 was used to generate the typical distributions, which are shown in Fig. 3. The lift coefficient distribution was obtained by adjusting the pitch of the hovering rotor theoretical model to yield the measured thrust. For the nominal condition of $C_T/\sigma = 0.07$, the adjusted pitch angle was 7.5 deg whereas the measured pitch angle was 6.9 deg, only a 0.6 deg difference. The drag coefficient distribution was predicted using the same free-wake model, but the integrated drag level was adjusted to match the measured torque on the rotor. For the same nominal condition, the measured level of torque ($C_Q/\sigma = 0.00604$) was one-third

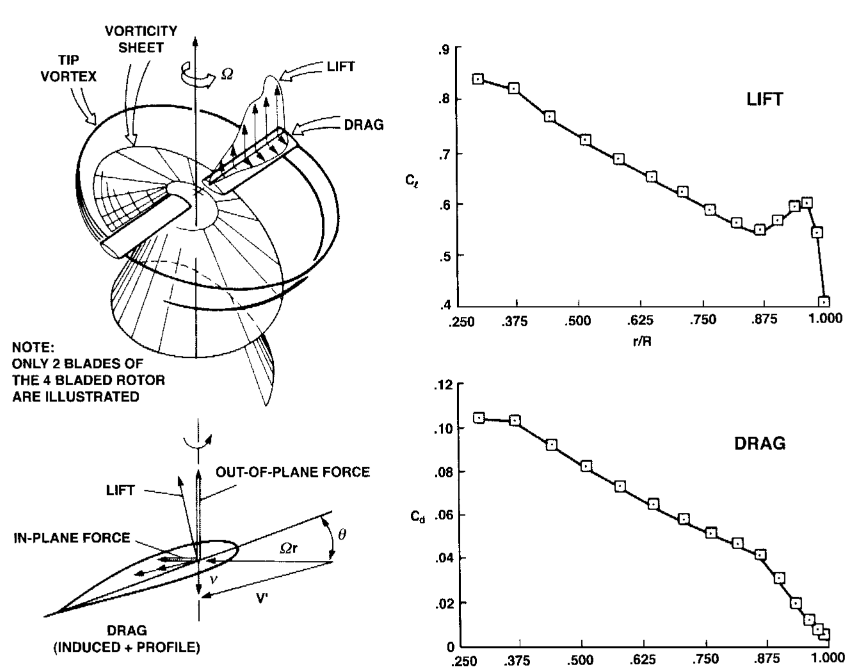

Fig. 3 Typical predicted aerodynamic loading distributions on a hovering rotor.

higher than the predicted value ($C_Q/\sigma = 0.00450$) showing the importance of correcting the theoretical model to match the measured data. Once these distributions and levels were determined, the local blade pressure forces were decomposed into out-of-plane forces (thrust) and in-plane forces (torque/radius) at each blade element, which were then used as known quantities in the second term of Eq. (1).

This procedure is really quite similar to Gutin's original analysis[2] except that the numerical evaluation is evaluated for a distribution of singularities along the radius instead of simple rotating point sources. Also, as stated earlier, Gutin's analysis does not consider the effects of thickness on the radiated noise.

The most straightforward computation of the radiated noise field is simply a direct numerical evaluation of Eq. (1). This was compared with a frequency-domain calculation in the acoustic far field (measurement distance of at least three diameters from the rotor) as illustrated in Fig. 2. Excellent agreement between the two separate evaluation methods is shown for the test case of the 360 hovering model-rotor for the microphone located 15 deg below the plane of the rotor and 4.6 diameters from the rotor hub. As shown, both of the linear theoretical prediction methods used in this paper have the same high fidelity and capture all of the important features of the noise radiation problem. This comparison of the two separate computer codes essentially validates them both and allows either to be used with confidence in the comparison with measured data. In the comparisons that follow, the theoretical predictions that are shown have been calculated using direct numerical evaluations of Eq. (1) (for details, see Ref. 16).

Experimental Measurements

The data shown in this paper were gathered in the DNW in a cooperative effort between the U.S. Army Aeroflightdynamics Directorate, the Boeing Helicopter Company, and NASA Ames Research Center in the summer of 1986. The test itself comprised a complete program of measuring the far-field noise and surface blade pressures on the Boeing 360 model helicopter rotor from hovering flight to high forward velocities. Only the low-frequency hovering noise data at selected microphones will be discussed in this paper.[17] A description of the high-speed portion of the program is given in Ref. 18; a comprehensive collection of all of the experimental acoustic data gathered in this test can be found in Ref. 19.

The Boeing 360 rotor is an advanced high-speed design that has also been optimized for good hover efficiency. It employs high-performance airfoils, nonlinear twist, and extensive taper in the tip region beginning at the 90% radial station. It has a hover design tip Mach number of 0.636 and is representative of a state-of-the-art helicopter rotor of the 1980s. Additional rotor design details are given in Ref. 17.

The hovering data were gathered with the DNW in the open-test-section mode. The 10-ft-diam model rotor was mounted on a series of extension housings on the DNW sting so that the rotor was positioned near the centerline of the tunnel out of ground effect (approximately 30 ft off the open-test-section floor). The installation is shown in Fig. 4.

The entire chamber that surrounds the open test section of the DNW is acoustically treated to eliminate echoes (making the chamber anechoic). In the far corners of the chamber, a simple bulk fiberglass treatment is used to cover the walls, and near the testing volume surrounding the open jet, a 1-m fiberglass wedge treatment is used over many of the wall surfaces. The collector lip is a fiberglass-screen construction, which also absorbs some acoustic energy. The collector and nozzle walls are made of steel, which tends to reduce the effectiveness of the anechoic space. The open-jet calibration of the DNW without a model in the test section is discussed in Ref. 20.

A scaled three-view sketch of the microphone arrangement reported in this paper is given in Figs. 5a–5c. Clusters of microphones at 1.5, 3.0, and 4.6 diameters from the rotor were used to ascertain the characteristic noise that emanates near the plane of the 360 rotor. The 1.5- and 3.0-diam microphone positions were located in the upstream tunnel direction; with the 3.0-diam position near the exit of the tunnel nozzle. The 4.6-diam microphone positions were

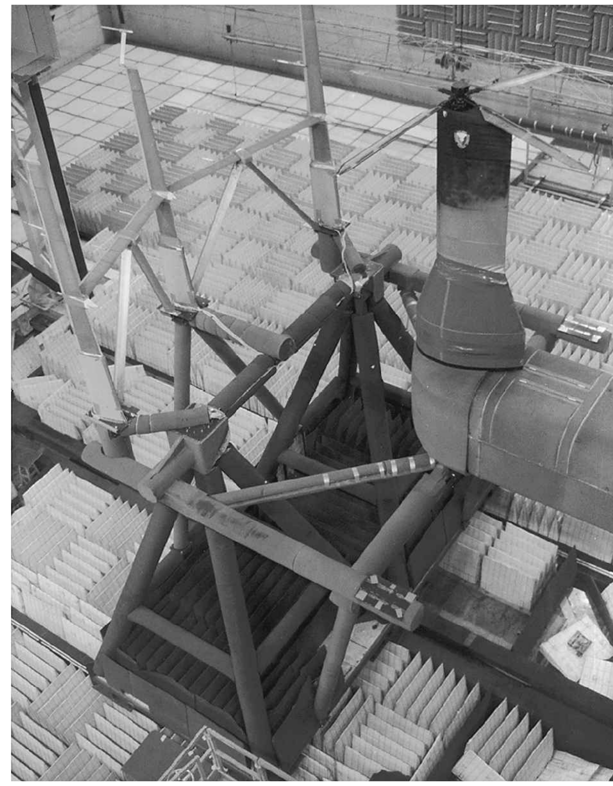

Fig. 4 Boeing 360 rotor mounted in the open-jet test section of the DNW wind tunnel.

located near the wall of the treated chamber in front of the 1-m fiberglass wedge treatment. Two additional microphones were located at 6.5 diameters from the rotor hub in the in-plane position near the corners of the measuring chamber.

Standard B & K microphones were used for this test. Microphones 1, 2, 14–17 were 0.25 in. (Type 4135) and equipped with UA0385 nose cones. Microphones 21–26 were 0.5 in. (Type 4133) with UA0237 windscreens.

A 32-channel Datacom/VAX751 system was used to digitize the microphone data with 15-bit (14 plus sign) resolution. A rotor-generated 1024/revolution clock was used so that 1024 points per revolution were acquired for each channel for a period of 32 revolutions. A rotor-generated 1/revolution was used to restart this sequence 32 times during each data run. In effect, a continuous time history of 32 revolutions was averaged 32 times for each data channel. Before digitizing, the analog acoustic signals were low-pass filtered to 1000 Hz. The analysis of the data was performed in both the time and frequency domains. Only the time-domain average time histories were used to validate the theory; they are shown in detail here. A comparison of the instantaneous and average time histories is shown in Figs. 6a and 6b for the in-plane microphone 1.5 diameter from the rotor hub. The average data are quite similar to the instantaneous time history, except for smaller unsteady variations that contribute less to the average over one rotor revolution. These smaller unsteady acoustic pressures are thought to be caused by the unsteady random pressure loading on the rotor. They become more important relative to the steady pressure terms for noise, which is measured close to the rotor thrust axis. This unsteadiness is known to be enhanced by recirculation of the rotor wake within the closed testing chamber.

Theory vs Experiment

The most direct method of comparing theory with experiment, simply comparing the average measured time-history data with time-history predictions, is presented in the following figures. To avoid near-field acoustic effects, only those microphones 3.0 diameters or farther from the rotor have been considered. Note that this method of comparing data in the time domain is much more

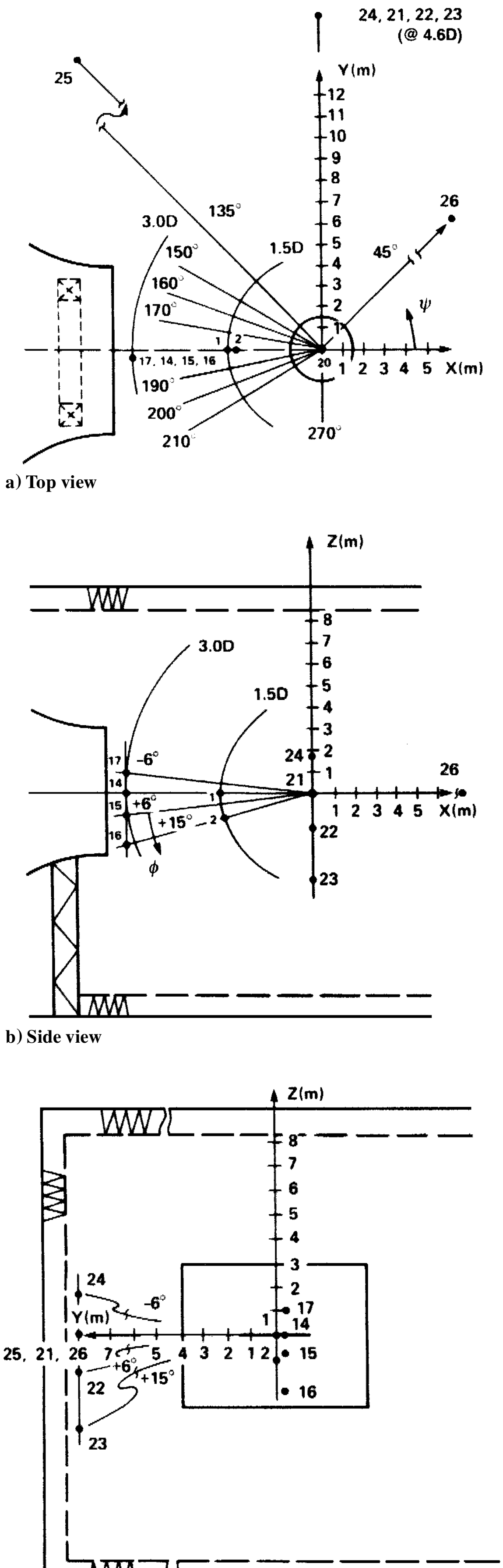

a) Top view

b) Side view

c) Downstream view

Fig. 5 Rotor and microphone locations in the open-jet test section of the DNW wind tunnel.

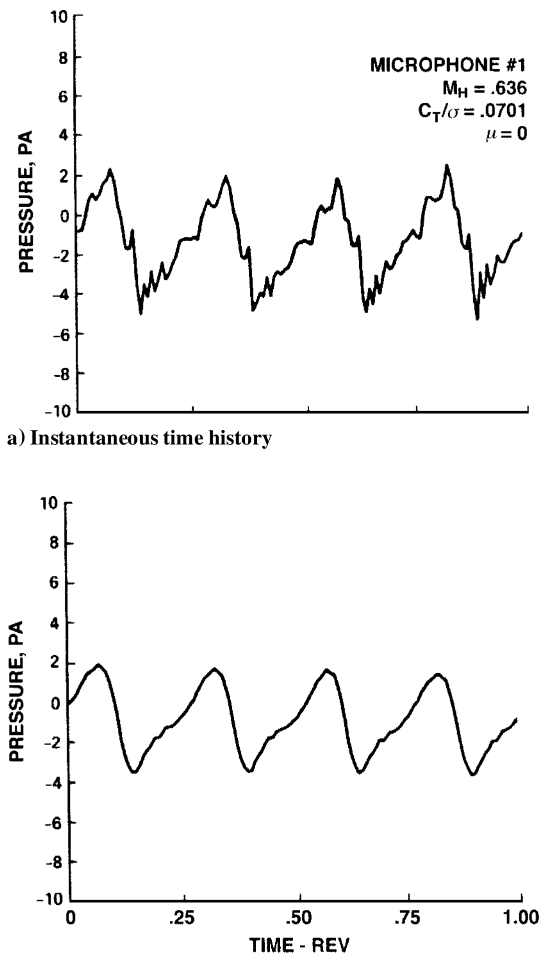

a) Instantaneous time history

b) Average (32) time history

Fig. 6 Typical measured time histories of acoustic pressure.

precise than simply comparing the amplitudes of harmonically analyzed data. The amplitudes and phases of the theory and the data are effectively compared by performing the comparison in the time domain.

The relative contributions of the thickness, drag, and thrust terms from linear acoustic theory for a microphone located at −6, 0, and +15 deg relative to the rotor plane and at a measurement distance of 3.0 diameters from the rotor hub is shown in Fig. 7. All three terms are seen to be important in the noise radiation process at this Mach number (0.636), which is typical of normal helicopter operation. Above the plane of the rotor (−6 deg), the contributions of thrust and drag tend to cancel, lowering the overall amplitude of the total pressure time history. In the plane of the rotor (0 deg), there is no thrust contribution to the radiated noise, whereas below the plane of the rotor (+15 deg), the contributions of thrust and drag tend to add, making the overall low-frequency signal grow in amplitude. Note that in general the force (thrust and drag) contributions are quite different from the thickness contribution to the acoustic time history. The thickness pulse is quite symmetric whereas the force pulses are not. This observation has been noted before by other researchers.[10,21]

Comparisons of theory and experiment on a radius of 3 diameters from the rotor hub are shown in Fig. 8. All four microphones shown are located quite close to the wind-tunnel nozzle, which is acoustically untreated. However, the amplitude comparison with the measured data at these microphone locations is fairly good. At the in-plane microphone position, which is in the center of the nozzle, the agreement with data is nearly perfect. Above and below the rotor plane, theoretical and measured pulse shapes do not agree as well, even though the overall amplitudes of the pulses agree quite well. At the 15-deg down microphone position, there is a notable discrepancy

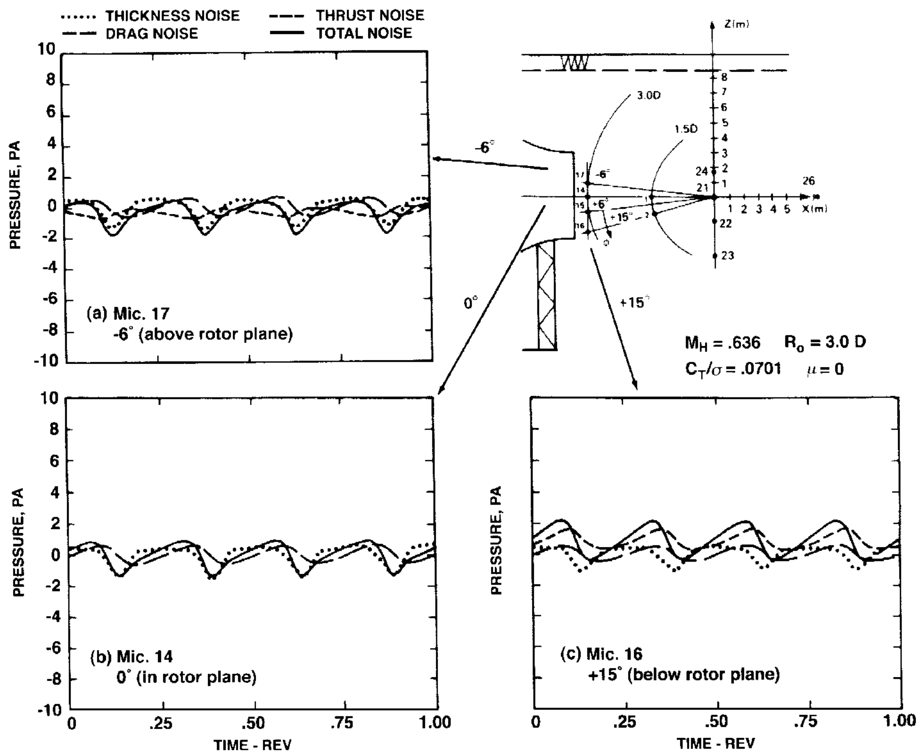

Fig. 7 Thickness and force contributions to predicted noise levels.

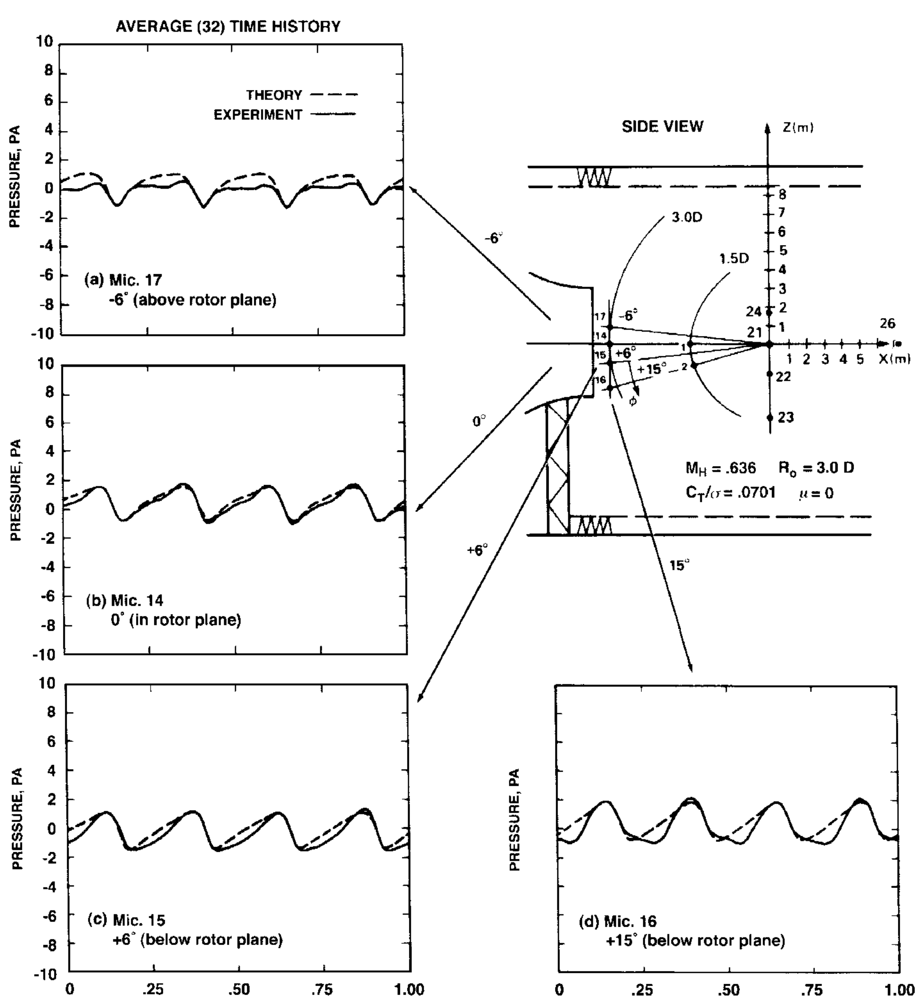

Fig. 8 Acoustic theory/experiment comparison at R/D = 3.0 (nominal condition).

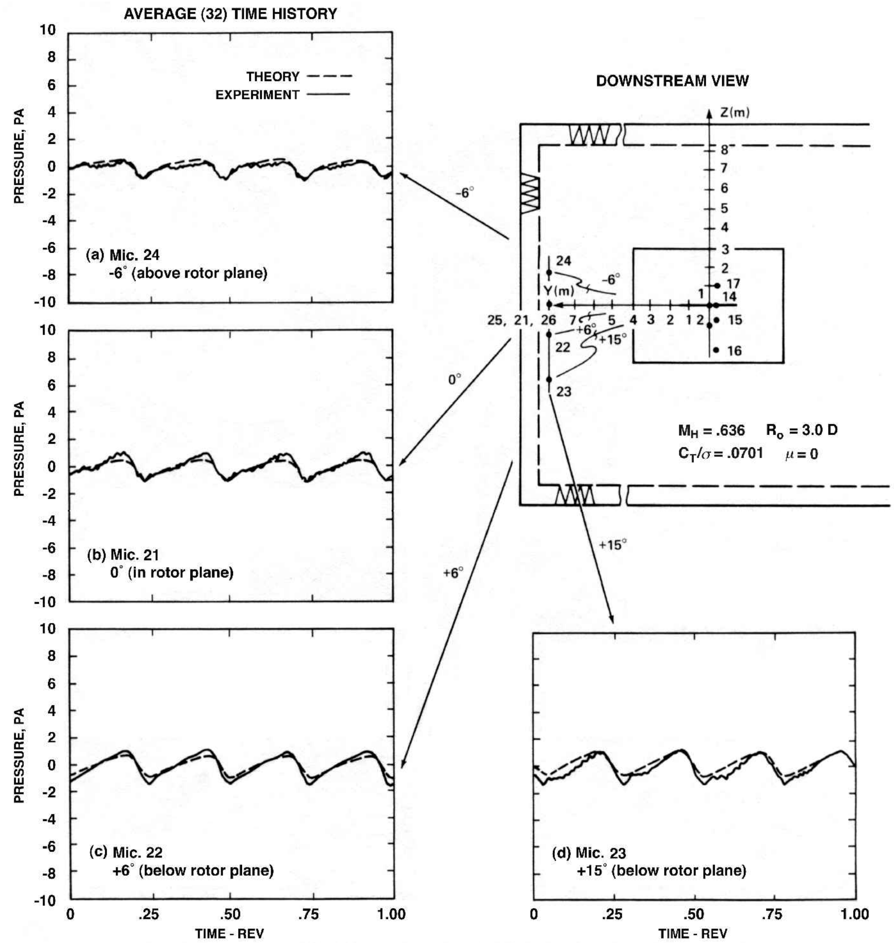

Fig. 9 Acoustic theory/experiment comparison at *R/D* = 4.6 (nominal condition).

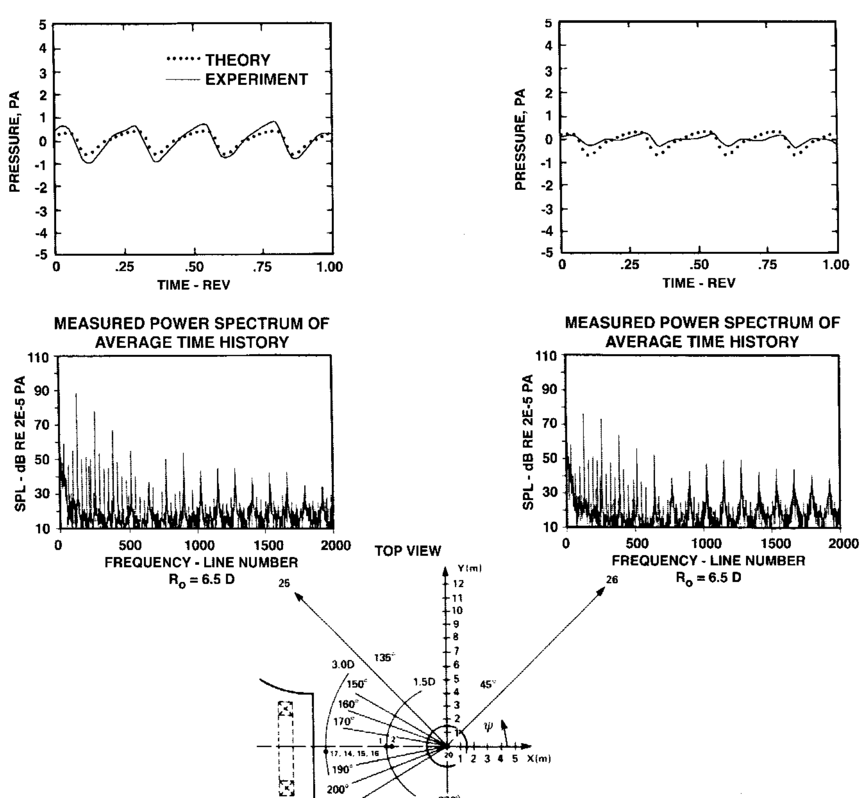

Fig. 10 Measured in-plane noise at a constant distance from the rotor (*R/D* = 6.5).

between the pulse shapes predicted by theory and that measured by the experiment. The closer proximity of the nozzle walls to the out-of-plane microphones is thought to be a contribution to the pulse shape discrepancies noted.

A similar comparison is made in Fig. 9 for the cluster of microphones located 4.6 diameters from the rotor hub in the part of the testing chamber with the most extensive acoustic treatment. The agreement of theory with data is much better at all of the microphone locations shown. The amplitudes and pulse shapes are predicted very precisely at the same elevation angles shown in Fig. 8.

A further comparison of theory and experiment is shown in Fig. 10 for the two in-plane microphones, which are located the farthest from the rotor (6.5 diameters from the rotor hub). Notably different acoustic amplitudes between the two experimental microphone positions are shown. At an azimuth angle of 135 deg, theory underpredicts the measured noise, and at an azimuth angle of 45 deg, theory overestimates the measured data. These two microphones are not located in the best part of the chamber for low-frequency measurements[20]; the 135-deg microphone is located in an area that is alongside of the untreated nozzle, and the 45-deg microphone is alongside the untreated part of the open-jet collector. It is likely that neither of these locations is sufficiently anechoic for these low-frequency acoustic signals, and they should not be used for theory validation.

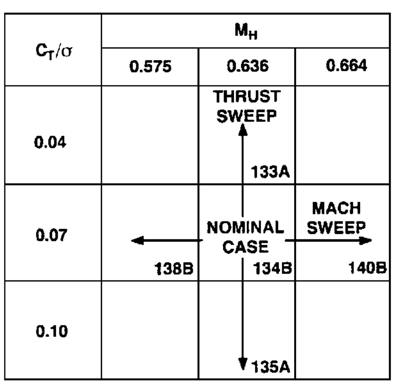

Fig. 11 Hovering 360 model-rotor noise test conditions.

Some very interesting conclusions can be drawn from these observations. Theory and experiment agree quite well for the Boeing 360 model-rotor tested in hover at this nominal condition at those microphones located in areas of the measurement chamber that are adequately treated acoustically. The pulse-shape changes that occur when the microphone is moved from above the plane of the rotor to below the plane are captured quite well by linear theory (Fig. 9). Thickness, thrust, and drag (torque) all contribute to the resulting time history. In each case, the amplitude of the overall pulse is predicted quite well.

It is also apparent that there is some distortion in the pulse shapes at a few microphone locations, the most notable being those microphones located near untreated surfaces of the open-jet wind tunnel. Similar effects were noted in Ref. 22 for a different wind tunnel. Measurements made away from these untreated surfaces show better correlation with theory. The unsteadiness of the rotor in the close measurement chamber, owing in part to possible recirculation effects, could alter the rotor inflow, thus inducing harmonic loading on the rotor that could distort the pulse shape in certain measurement positions. To check for this possibility, selected hover blade pressure measurements were reviewed to look for a connection between unsteady blade pressures and radiated noise. Unfortunately, because both rotor unsteadiness and reduced anechoic conditions at low frequencies can distort the measured acoustic pulse, it is a very difficult task to try to assess the relative importance of each separate effect. However, a recent review of these pressures indicated that the variations in blade surface pressures that did occur were random in phase. This makes the unsteady pressure variations unlikely distortions of the averaged noise data.

Figure 11 presents a matrix of test conditions that were chosen for further validation studies. A hover tip Mach number sweep from 0.575 to 0.664 at a nominal thrust coefficient/solidity ratio of 0.07 is shown in Fig. 12 for the in-plane microphone position near the center of the nozzle. Very good agreement with data is shown, for both amplitude and phase, over the entire Mach number range. The peak amplitude levels tend to be slightly underpredicted at the higher Mach numbers, a result that is consistent with other measured data.[9] The underprediction in level is slight, not the factor of two reported in the literature for older, thicker helicopter rotors operating at higher rotational Mach numbers.

The effect of thrust-level changes on low-frequency radiated noise levels is shown in Fig. 13. The position at 15 deg below the rotor

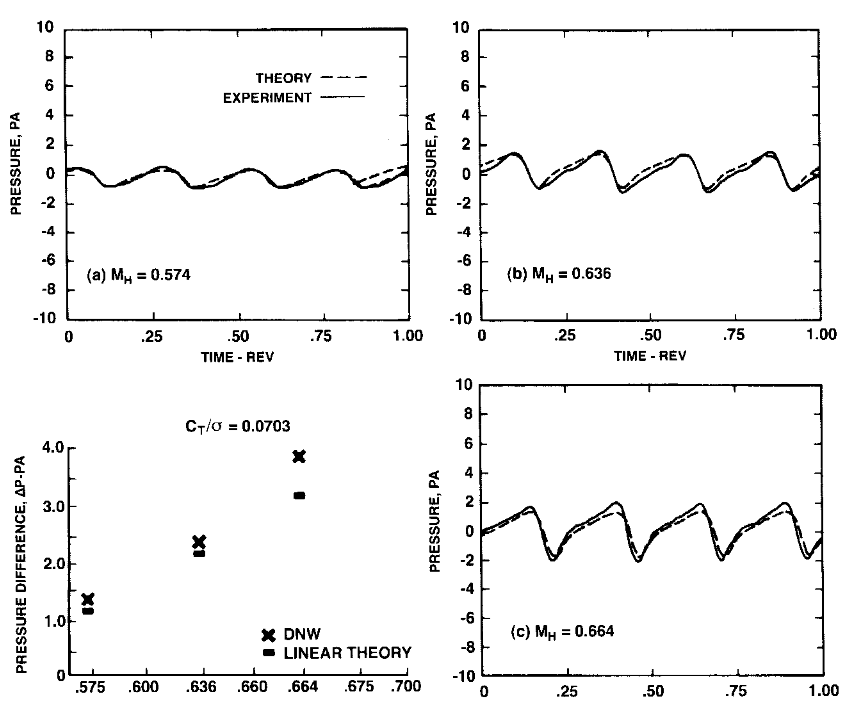

Fig. 12 Acoustic theory/experiment validation at different Mach numbers (in-plane microphone).

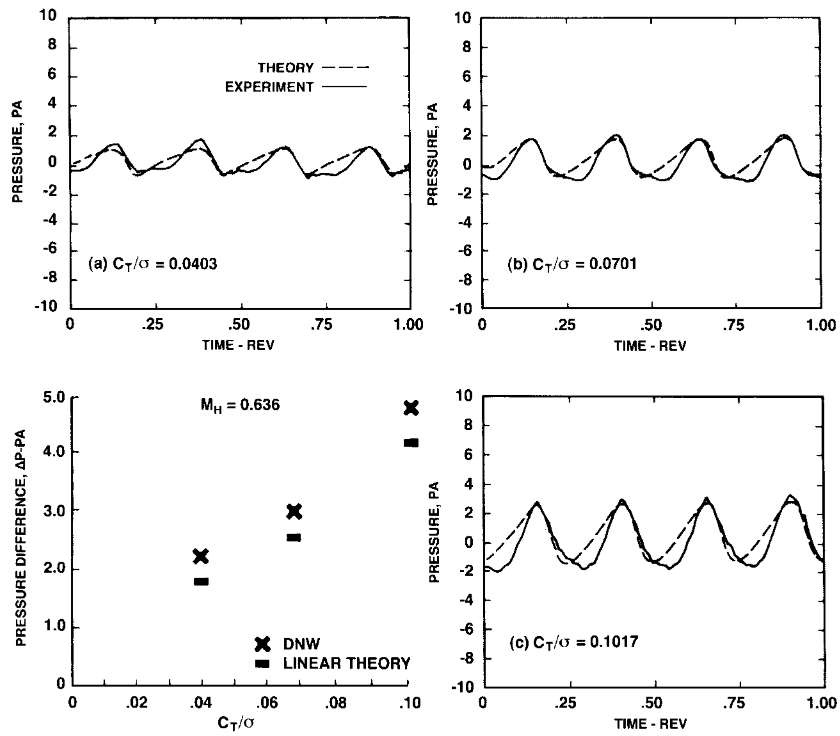

Fig. 13 Acoustic theory/experiment validation at different thrusts (15 deg below the rotor plane).

plane was chosen for this comparison because at this location the measured acoustic pressure is more dependent on the effects of thrust than are the in-plane microphone positions. Unfortunately, at this measurement position, the pulse shape is distorted somewhat (Fig. 8), probably due to reflections from the nearby untreated tunnel nozzle. As shown in Fig. 13, the measured wave shape at this location makes the pulse-shape comparisons consistently in error in the time domain. In spite of these consistent local distortions, linear theory does well in predicting the amplitude of the acoustic pressure over the entire thrust range.

Conclusions

Careful testing of a hovering model helicopter rotor in an acoustically treated chamber (the DNW open-jet wind tunnel) has shown that classical linear acoustic theory accurately predicts the near in-plane average amplitude level and shape of low-frequency harmonic rotor noise of the Boeing 360 model-rotor. Thickness (monopole) and pressure (dipole) terms are equally important in the acoustics computations over the hovering tip Mach number range of 0.575–0.664. Each term has its characteristic waveform, which must be summed with the correct phase to predict accurately the measured acoustic pressure time history. At the higher hover tip Mach number, theory tends to slightly underpredict the measured noise levels for this modern four-bladed model rotor.

The importance of having high-quality measurements with which to validate acoustic prediction codes has been demonstrated. Details of the pressure-time history are quite dependent on the quality of the anechoic space in which the measurements are taken. It is necessary to have a measurement chamber with sufficient acoustic treatment in the low-frequency range of interest to be able to quantitatively validate theory. For low-frequency harmonic model rotor noise caused by steady loading and thickness, acoustic measurements taken in the best anechoic parts of the chamber, away from untreated surfaces, show the best correlation with theory.

The cause of small differences in phase at some microphone positions between theory and experiment are difficult to resolve. Although the unsteadiness of a hovering rotor in a closed chamber and reduced anechoic conditions at low frequencies are possible contributors to this discrepancy, the latter effect is thought to be responsible the majority of the phase distortion.

Acknowledgment

The authors would like to thank Chee Tung for his help computing the free-wake lift and drag distributions for the Boeing 360 model rotor described in the paper.

References

[1]Hubbard, H., and Lassiter, L., "Sound from a Two-Bladed Propeller at Supersonic Tip Speeds," NACA Rept. 1079, 1952.

[2]Gutin, L.,"On the Sound Field of a Rotating Propeller," *Physikalische Zeitschrift der Sowjetunion*, Vol. 9, No. 1, 1936, pp. 57–71 (translated from Russian to English in NACA TM-1195, Oct. 1948).

[3]Leverton, J., "The Noise Characteristics of a Large Clean Rotor," *Journal of Sound and Vibration*, Vol. 27, No. 3, 1973, pp. 357–376.

[4]Brown, D., and Ollerhead, J. B., "Propeller Noise at Low Tip Speeds," TR AFAPL-TR-71-55, Wyle Lab., Hampton, VA, Sept. 1971.

[5]Sternfeld, H., Spencer, R., and Schairer, J., "An Investigation of Noise Generation on a Hovering Rotor," TR DZ10-10550-1, U.S. Army Research Office, Durham, NC, Jan. 1971.

[6]Reynolds, D., Janakiram, D., and Corban, J., "Main Rotor Noise Dominant MD-500E Helicopter-Ground Tests," NASA CR 178318, July 1987.

[7]Robinson, F., "Component Noise Variables of a Light Observation Helicopter," NASA CR 114761, 1973.

[8]Hosier, R., and Ramakrishnen, R., "Helicopter Rotor Rotational Noise Predictions Based on Measured High-Frequency Blade Loads," NASA TND-7624, 1974.

[9]Watts, M. E., and Jordan, D. J., "Acoustic Results of the Boeing Model 360 Whirl Tower Test," 16th European Rotorcraft Forum, Glasgow, Scotland, U.K., 1990, pp. II.3.2.1–II.3.2.11.

[10]Boxwell, D. A., Yu, Y. H., and Schmitz, F. H., "Hovering Impulsive Noise: Some Measured and Calculated Results," *Vertica*, Vol. 3, 1979, pp. 35–45; also NASA CP-2052, 1978.

[11]Lorber, P. F., "Blade–Vortex Interaction Data Obtained from a Pressure-Instrumented Model UH-60A Rotor at the DNW," *Journal of the American Helicopter Society*, Vol. 38, No. 3, 1993, pp. 26–34.

[12]Visintainer, J. A., Marcolini, M. A., Burley, C. L., and Liu, S. R., "Acoustic Prediction Using Measured Pressures from a Model Rotor in the DNW," *Journal of the American Helicopter Society*, Vol. 38, No. 3, 1993, pp. 35–44.

[13]Splettstoesser, W. R., Kube, R., Wagner, W., Seelhorst, U., Boutier, A., Micheli, F., Mercker, E., and Pengel, K., "Key Results from a Higher Harmonic Control Aeroacoustic Rotor Test (HART)," *Journal of the American Helicopter Society*, Vol. 42, No. 1, 1997.

[14]Ffowcs-Williams, J. E., and Hawkings, D. L., "Sound Generation by Turbulence and Surfaces in Arbitrary Motion," *Philosophical Transactions of the Royal Society of London, Series A: Mathematical and Physical*

Sciences, Vol. 264, May 1969, pp. 321–342.
[15]Summa, J., "Advanced Rotor Analysis Methods for the Aerodynamics of Vortex-Blade Interactions in Hover," *Vertica*, Vol. 9, No. 4, 1985, pp. 331–343.
[16]Aggarwal, H. R., "Low-Frequency Helicopter Acoustic Prediction," Final Rept., Aeroflightdynamics Directorate Contract NAS 2-12239, NASA Ames Research Center, Moffett Field, CA, March 1988.
[17]Boxwell, D. A., "Low-Frequency Narrowband Analysis of the Boeing Vertol Model 360 Rotor Acoustic Signatures in Hover and Low-Speed Forward Flight," AATMR TR 87-1, Vol. 1 and 2, U.S. Army Aeroflightdynamics Directorate, NASA Ames Research Center, Moffett Field, CA, Jan. 1987.
[18]Dadone, L., Dawson, S., and Ekquist, D., "Model 360 Rotor Test at DNW– Review of Performance and Blade Airload Data," 43rd Annual Forum of the American Helicopter Society, St. Louis, MO, 1987.
[19]Boxwell, D. A., Zinner, R. A. and Kodani, H. M., "Boeing Vertol Model 360 Rotor Acoustic Signature Measurements in the DNW," AATMR TR 88-1–88-11, U.S. Army Aeroflightdynamics Directorate, NASA Ames Research Center, Moffett Field, CA, June 1988.
[20]Van Ditshuizen, J. C. A., Ross, R., and Schultz, K. J., "Acoustic Capabilities of the German-Dutch Wind Tunnel (DNW)," AIAA Paper 83-0146, Jan. 1983.
[21]Aggarwal, H. R., "Helicopter Noise as Predicted by Three-Dimensional Monopole and Quasi-Steady Full Potential Dipole Sources," *Proceedings of the 9th Aeroacoustics Conference*, Williamsburg, VA, Oct. 1984.
[22]Schmitz, F., Boxwell, D., Lewy, S., and Dahan, C., "Model-to-Full-Scale Comparisons of Helicopter Blade–Vortex Interaction Noise," *Journal of the American Helicopter Society*, Vol. 29, No. 2, 1984, pp. 16–25.